Journal of the European Ceramic Society 37 (2017) 923–930

Contents lists available at www.sciencedirect.com

Journal of the European Ceramic Society

journal homepage: www.elsevier.com/locate/jeurceramsoc

The effect of z value on intergranular phase crystallization of α^1/β^1-SiAlON-TiN composites

Nurcan Calis Acikbas [a,*], Ferhat Kara [b]

[a] Department of Metallurgical and Materials Engineering, Bilecik S.E. University, Bilecik, Turkey
[b] Department of Materials Science and Engineering, Anadolu University, Eskisehir, Turkey

ARTICLE INFO

Article history:
Received 22 July 2016
Received in revised form 7 October 2016
Accepted 8 October 2016
Available online 13 October 2016

Keywords:
SiAlON-TiN composites
z value
Microstructure
Crystallization
Cutting tool

ABSTRACT

Relationship between z value and intergranular phase (IGP) chemistry has not been completely developed to date for SiAlON based materials. In this study, the effect of z value of β^1-SiAlON on crystallization and coalescence of IGP was investigated in α^1/β^1-SiAlON doped with Yb_2O_3-Sm_2O_3-CaO sintering additives and reinforced with TiN particles. α^1/β^1-SiAlON-TiN composites with compositions yielding different z values (0.3, 0.5, 0.7, 0.9 and 1.1) were prepared and sintered with gas pressure sintering route. Post sintering heat treatment was applied to sintered samples in order to enhance crystallization and coalescence of IGP. z value was proved an effective parameter on the intergranular phase chemistry and crystallization which are further influenced by post sintering heat treatment. No noticeable influence of heat treatment was observed on mechanical properties.

1. Introduction

High technology ceramics have been used as cutting tools in metal machining for over 30 years [1]. Silicon nitride (Si_3N_4) and alumina based (Al_2O_3-SiC_w) ceramics have been widely used for cast iron and nickel based super alloy machining, respectively. Although SiAlON ceramics have been used in super alloy machining at lower cutting speeds, Al_2O_3-SiC_w cutting tools are main choice of cutting materials due to their higher performance at higher cutting speeds. However Al_2O_3-SiC_w cutting tools are produced by hot pressing technique which is a costly production method and SiC whiskers are dangerous to human health [2,3]. On the other hand SiAlON based cutting tools can be produced by gas pressure sintering technique which is more suitable to serial production and these tools have a cost advantage over Al_2O_3-SiC_w cutting tools. Therefore, there is an interest to develop the performance of SiAlON ceramics to extend their applications in superalloy machining.

Superalloys are rather difficult to machine materials due to their high hot hardness, strength and ductility and also to the presence of abrasive hard carbides (for example; MC, M23C6) leading to wear and fracture of cutting tool [4–9]. There may be two ways to improve cutting performance of SiAlONs for superalloy machining: Tailoring SiAlON microstructures and addition of reinforcement phases. Our initial studies on machining of superalloys by SiAlONs addressed the effect solid solution parameter (z) on cutting performance [10]. The study showed that z value was very effective parameter on cutting performance. z value represents the substitution of Al-O for Si-N in the β^1-$Si_{6-z}Al_zO_zN_{8-z}$ crystal structure and can be varied continuously from 0 to 4.2 [11–13]. Low z value β^1-SiAlON (e.g. 0.2–0.3) have a short tool life in superalloy machining because of chemical wear during machining, although they have better mechanical properties like toughness [14,15].

The key parameters that affect the cutting tool life during super alloy machining are high hardness, wear resistance, chemical inertness and fracture toughness. Therefore TiN is a very good candidate to impart these properties to SiAlON matrix. In our previous studies, the effect of TiN (average particle size of 1–2 μm) addition on the densification, phase assemblage, microstructural evolution, z value and thermal shock resistance of α^1/β^1-SiAlON compositions were investigated [16,17]. It was determined that TiN addition did not have any adverse effect on densification, phase assemblage, z value and mechanical properties. The microstructure of α^1/β^1-SiAlON-TiN composites consisted of elongated β^1-SiAlON grains and the fracture toughness increased with the increasing TiN amount with no prominent change in the hardness. The composites exhibited a superior thermal shock property when the amount of TiN was 25 wt%. The addition of TiN particles into SiAlON matrix is a cost

* Corresponding author.
E-mail address: nurcan.acikbas@bilecik.edu.tr (N.C. Acikbas).

http://dx.doi.org/10.1016/j.jeurceramsoc.2016.10.006
0955-2219/

effective way of increasing thermal conductivity, chemical wear resistance and reduction in brittleness.

SiAlON ceramics are sintered with the help of a liquid phase due to their covalent nature and this liquid phase remains at intergranular regions forming a low melting temperature zones compared to SiAlON matrix phase. Due to local temperature rise at the tip of the cutting tool during machining, it is expected that crystallization of these regions should lead to an increase in machining performance due to increased hot hardness and strength [18].

It is clear that z value and IGP crystallization relationship is an important subject that needs to be investigated in SiAlON based material production. Both high z value and crystalline intergranular phase may have a positive effect on chemical wear resistance of α^1/β^1-SiAlONs, especially, at high temperatures. Therefore, in our previous study, the primary target was to determine the effect of cation type, intergranular phase amount and cation mole ratios on z value and intergranular phase crystallization of SiAlONs [16]. It was found that, Yb containing system had higher crystallization tendency in comparison to Er and Y containing system. Therefore, in this study Yb:Sm:Ca cation system was selected for the purpose of determining the effect of z value (between 0.3–1.1) on the crystallization of intergranular phase. Along with the crystallization of intergranular phase, its coalescence behaviour may be important for high temperature properties. For this purpose post sintering heat treatment was applied to the samples, enhancing the liquid phase diffusion along the grain boundaries which in turn led to the coalescence of submicron triple junctions into larger pockets where crystallization readily occurred. Increased crystallinity and coalescence of the intergranular phase is expected to reduce the chemical reaction tendency of the cutting tool with the work piece which would result in less wear.

In our previous study in Y:Sm:Ca doped α^1/β^1–SiAlONs, the effect of post sintering heat treatment time between 2 and 6 h was studied at 1600 °C and 2 h heat treatment time was found to be sufficient to obtain substantial crystallization of intergranular phase into melilite [19]. In another preliminary study, α^1/β^1-SiAlON composition with 0.2 z value were designed with Er:Sm:Ca cation system and the effect of heat treatment temperatures (1500 °C, 1600 °C, 1700 °C, 1750 °C and 1800 °C) on crystallization was investigated. It was found that 1700 °C for 2 h is the most effective on crystallization and coalescence of intergranular phase. Therefore, in this study temperature and duration of the heat treatment were chosen as 1700 °C and 2 h, respectively.

The purpose of this study is to evaluate the effect of z value on the crystallization of IGP and microstructural development in an α^1/β^1-SiAlON containing TiN particles which is aimed to be developed for cutting tool application for superalloys. Furthermore, correlation was made between z value and the coalescence behaviour of IGP on heat treatment.

2. Experimental procedures

In order to obtain high hardness and high toughness $25\alpha^1:75\beta^1$ SiAlON composition with 17 wt% TiN particle addition was produced with different z values (0.3, 0.5, 0.7, 0.9 and 1.1, designated as Z03, Z05, Z07, Z09 and Z11, respectively) with 9Yb:0.5Sm:0.5Ca cation system and% 2 mol IGP content (see Table 1). The general formula of α^1-SiAlON is $M_xSi_{12-(m+n)}Al_{m+n}O_nN_{16-n,}$ where M is stabilizing cation like Li, Mg, Ca,Y, rare earth elements except for La, Ce, Pr and Eu. x is equal to m divided by the valency of the M cation. The m index expresses the amount of Si-N bonds replaced by longer Al-N bonds, depends on the valence of the M cation and x value. $25\alpha^1:75\beta^1$ SiAlON composition was formulated with nominal n = 1.3 and m = 1.25 has the *x* value of 0.416 (x = m/3). The chemical composition of raw material for the processing of SiAlON ceramics is as follows: High purity α-Si_3N_4 powder (E-10 grade, UBE Co. Ltd., Japan) with 1.4 wt% O content, high purity AlN powder (H Type, Tokuyama Corp. Japan) containing 1.6 wt% O, Al_2O_3 (Alcoa A16-SG, Pittsburgh, USA), Yb_2O_3 (> 99.99%, Treibacher, Austria), Sm_2O_3 (>99.9%, Stanford Materials Corp., USA), $CaCO_3$ (>99.75%, Reidel-de Haen, Germany) and TiN powder with average particle size of 1–2 μm (> 99% pure, H.C. Starck, Grade C, Berlin, Germany).

The slurries with the above compositions were prepared by planetary milling for 90 min at 300 rpm in isopropyl alcohol using Si_3N_4 balls. The slurries were then dried using a rotary evaporator and sieved with a mesh size of 250 μm. The powders were uniaxially pressed to a maximum pressure of 25 MPa, and subsequently cold isostatically pressed at 300 MPa to increase green density. The pellets were sintered using a two-step gas pressure sintering cycle. The first step (pre-sintering) was carried out at 1840 °C for 60 min at 0.5 MPa nitrogen gas pressure followed by sintering step at 1890 °C for 90 min at 2.2 MPa nitrogen gas pressure and then the furnace was allowed to cool at a rate of 5 °C/min. In order to increase crystallization and coalescence of intergranular phase, post sintering heat treatment was applied to sintered samples at 1700 °C for 2 h under 0.5 MPa nitrogen gas pressure.

Relative bulk density, measured by the Archimedes principle was over >99.5%. The types of crystalline phases and the $\alpha^1:\beta^1$-SiAlON phase ratios were determined by means of X-ray diffraction analyses (XRD-Panalytical, Empyrean with Cu-Kα radiation). The $\alpha^1:\beta^1$-SiAlON phase ratios were found by quantitative estimation from the XRD patterns using the integrated intensities of the (102) and (210) reflections of α^1-SiAlON and the (101) and (210) reflections of β^1-SiAlON by the following equation:

$$\frac{I_\beta}{I_\beta + I_\alpha} = \frac{1}{1 + K\left[\left(1/w_\beta\right) - 1\right]} \quad (1)$$

where I_α *and* I_β are observed intensities of α^1 and β^1-SiAlON peaks, respectively, w_β is the relative weight fraction of β-SiAlON, and K is the combined proportionality constant resulting from the constants in the two equations, namely:

$$I_\beta = K_{\beta *} W_\beta \quad (2)$$

$$I_\alpha = K_{\alpha *} W_\alpha \quad (3)$$

which is (0.518 for β (101) − α (102) reflections and 0.544 for β (210) − α (210) reflections [20].

The cell parameters of β^1-SiAlON were measured with silicon powders as the internal standard. The z-value of the β-SiAlON phase was obtained from the mean of z_a and z_c values given by the following equations:

$$z_a = \frac{a - 7.6044}{0.031} \quad (4)$$

$$z_c = \frac{c - 2.9075}{0.026} \quad (5)$$

where *a* and *c* are the calculated unit cell dimensions of β^1-SiAlON: JCPDS card 33–1160 was used as a reference for β-Si_3N_4 where a = 7.6044(2)Å and c = 2.9075(1)Å.

The microstructural investigation of the polished surfaces of sintered and heat treated samples was performed by means of a

Table 1
Designed SiAlON-TiN compositions with different z values.

Sample	Cation Molar Ratios	*Aimed z values*	*Intergranular Phase Content (molar%)*
Z03	9Yb:0.5Sm:0.5Ca	0.3	2.00
Z05	9Yb:0.5Sm:0.5Ca	0.5	2.00
Z07	9Yb:0.5Sm:0.5Ca	0.7	2.00
Z09	9Yb:0.5Sm:0.5Ca	0.9	2.00
Z11	9Yb:0.5Sm:0.5Ca	1.1	2.00

scanning electron microscope (SEM-ZEISS Supra 40VP) by using back-scattered electron imaging mode.

The hardness (HV10) and indentation fracture toughness (K_{1C}) at room temperature were obtained with a Vickers diamond indenter, using a 98 N load. The Vickers hardness (HV) was calculated by the following equation (Evans and Charles) [21]:

$$HV_{10} = 0.47P/a^2 \quad (6)$$

where, HV_{10} is the Vickers hardness, P is load applied and a is half the length of the diagonal of the indentation produced by the indenter. The fracture toughness (K_{1C}) has been measured by using the indentation fracture (IF) toughness technique. In this study, the indentation fracture toughness K_{1C} ($MPam^{1/2}$) was calculated using the formula proposed by Niihara et alfor median cracks [22]:

$$K_{IC} = 0,018 * HV * a^{0,5} * (E/HV)^{0,4} * (c/a-1)^{-0,5} (for c/a < 3.5 and l/a < 2.5) \quad (7)$$

where 2a is the average indent diagonal length (μm), 2c is the crack length (from one crack tip to another), E is the elastic modulus (GPa) which is taken as a constant equivalent to 320 GPa for all the samples and H is the measured hardness (GPa). Both the indent diagonal and crack length were carefully measured from optical images of the indented surfaces and the reported hardness and fracture toughness values were the average of at least five indentation measurements. 3 samples tested for per composition with 5 indents and standard deviation was calculated.

3. Results and discussion

3.1. The effect of z value on crystallization of as-sintered SiAlONs

The XRD analysis after sintering showed that desired 75β¹:25α¹ phase ratios were almost obtained in all samples which have different z values (see Table 2). The SiAlON samples which had lower designed z values ($z \leq 0.5$) had higher z values than the designed ones. On the other hand, the SiAlON samples which had higher designed z values ($z \geq 0.7$) showed lower z values than the designed ones (Table 2). The difference was attributed to the intergranular phase chemistry as such that in order to obtain high z values "aluminium" content in the SiAlON composition had to be increased when designing compositions. Aluminium was introduced by adding Al_2O_3 and AlN into the compositions. With increasing Al_2O_3 and/or AlN addition, aluminium cation caused the formation of high alumina containing aluminate phase ($Yb_3Al_5O_{12}$) crystallization as a grain boundary phase and this consumed some of the aluminium that should have been incorporated into the Si_3N_4 crystal structure (Fig. 1).In the case of the SiAlON samples with lower designed z value, Jss phase (woehlerite) phase formation occurred and this does not consume alumina as much as the aluminate phase and thus more aluminium was available to be incorporated into the Si_3N_4 crystal structure causing slightly higher z value than the designed.

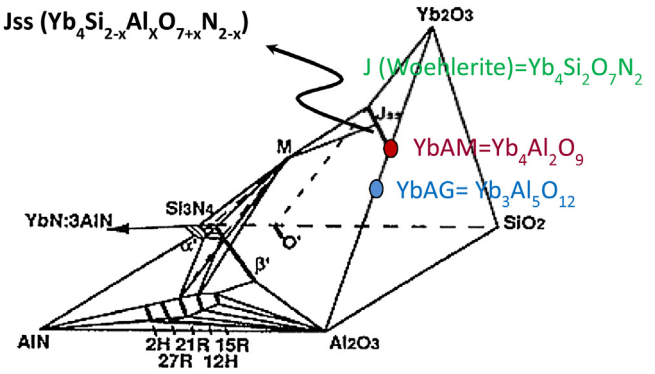

Fig. 2. Phase relationship of Yb-Si-Al-O-N system [23].

The SiAlON samples with z value between 0.43 and 0.74, Jss phase ($Yb_4Si_{2-x}Al_xO_{7+x}N_{2-x}$) located between J phase ($Yb_4Si_2O_7N_2$) and YbAM phase ($Yb_4Al_2O_9$) tie line was observed. Aluminate ($Yb_3Al_5O_{12}$) phase crystallization was obtained in the Z11 sample (Note that peaks at 21° 2θ and 28.2° 2θ of $Yb_3Al_5O_{12}$ was used to separate Jss and $Yb_3Al_5O_{12}$ phases). Phase relations of Yb-Si-Al-O-N system were given in Fig. 2 [23]. In the literature it is stated that with increasing Al_2O_3 solubility in Jss, oxidation resistance is enhanced [24]. Therefore, alumina containing woehlerite solid solution was considered as a favorable intergranular phase for SiAlON ceramics. Stability of alumina containing RE-woehlerite solid solution increased with decreasing RE ionic radius (e.g. Yb_2O_3). Woehlerite phase crystallized readily during cooling from the liquid phase, and hence, it had higher degree of crystallization than in the case of devitrification of glasses by means of post sintering heat treatments [25]. Woehlerite phase does not form low eutectic temperature with Si_3N_4 and so possesses much better refractoriness and stability up to 1350 °C. It was reported to have as good mechanical properties as N-melilite phase [23]. On the other hand, $Yb_3Al_5O_{12}$

Table 2
Phase evolution, z values and IGP crystallization, coalescence behaviour and mechanical properties of sintered SiAlON-TiN composites (Jss:$Yb_4Si_{2-x}Al_xO_{7+x}N_{2-x}$, YbAG: $Yb_3Al_5O_{12}$).

	Z03	Z05	Z07	Z09	Z11
β:α¹ SiAlON ratio	71β: 29α	73β: 27α	73β: 27α	76β: 24α	77β: 23α
z value	0.43	0.55	0.57	0.74	0.91
IGP composition	Jss (I_{Jss}/I_β:0.18)	Jss (I_{Jss}/I_β:0.05)	Jss (I_{Jss}/I_β:0.027)	Jss (I_{Jss}/I_β:0.019)	YbAG (I_a/I_β:0.017)
HV10 (GPa)	16.76 ± 0.20	16.70 ± 0.50	16.50 ± 0.20	15.79 ± 0.36	15.74 ± 0.07
Kıc ($MPam^{1/2}$)	7.50 ± 0.10	7.20 ± 1.03	7.10 ± 0.20	6.97 ± 0.16	6.90 ± 0.25

Table 3
Phase evolution, z values and IGP crystallization, coalescence behaviour and mechanical properties of heat treated SiAlON-TiN composites (Jss:$Yb_4Si_{2-x}Al_xO_{7+x}N_{2-x}$, YbAG: $Yb_3Al_5O_{12}$).

	Z03	Z05	Z07	Z09	Z11
β¹:α¹ SiAlON ratio	73β: 27α	71β: 29α	73β: 27α	76β: 24α	80β: 20α
z value	0.30	0.46	0.59	0.80	0.97
IGP composition	Jss (I_{Jss}/I_β:0.19)	Jss (I_{Jss}/I_β:0.17)	Jss and YbAG (I_{Jss}/I_β:0.042 I_a/I_β:0.019)	YbAG (I_a/I_β:0.06)	YbAG (I_a/I_β:0.1)
HV10 (GPa)	16.86 ± 0.2	16.50 ± 0.25	16.40 ± 0.20	16.22 ± 0.41	15.84 ± 0.32
Kıc ($MPam^{1/2}$)	7.09 ± 0.17	6.64 ± 0.17	6.98 ± 0.05	6.55 ± 0.05	6.65 ± 0.20

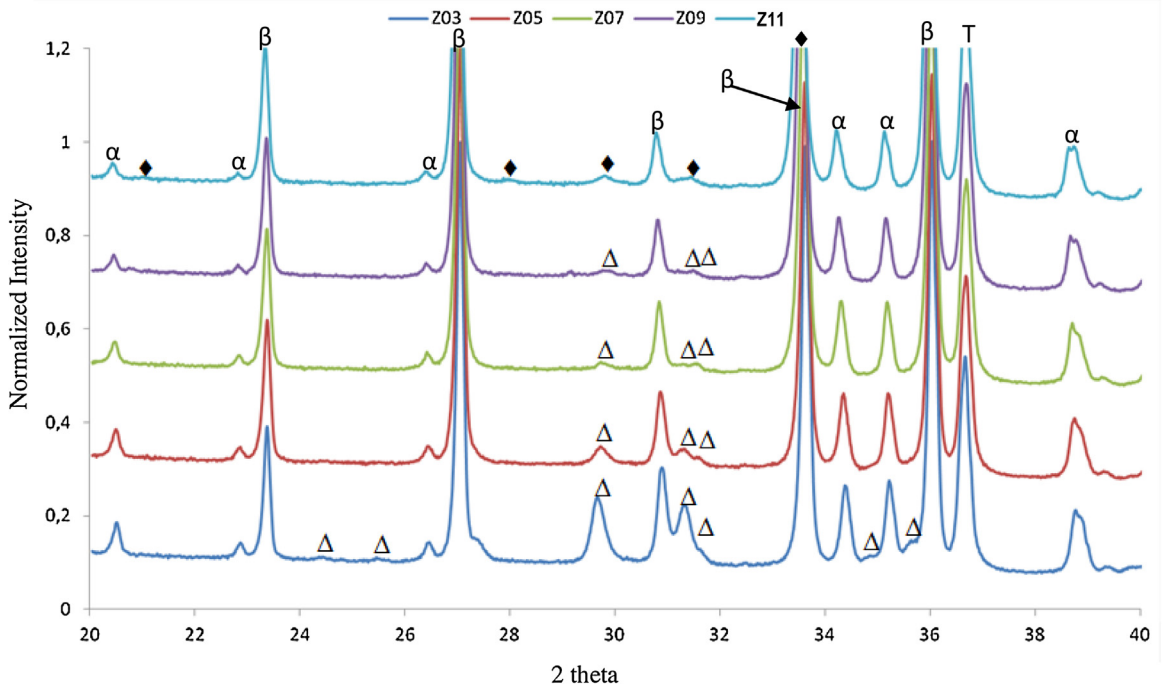

Fig. 1. XRD pattern of assintered SiAlON-TiN composites which have different z values (β¹:Beta SiAlON phase, α¹:Alpha SiAlON phase, T:TiN; Δ:Jss- $Yb_4Si_{2-x}Al_xO_{7+x}N_{2-x}$;♦: $Yb_3Al_5O_{12}$).

phase rich in oxygen was reported to have better oxidation resistance [24].

Z03 sample had a good crystallization tendency while all the other samples had no appreciable crystallization after sintering (Table 2). Although, the calculation of α¹: β¹ content in Si_3N_4 based materials is well documented [26], it is in general difficult to quantify crystalline intergranular phase content. Therefore, the relative amount of Jss phase was calculated by dividing the Jss peak intensity at the interplanar spacing of $d = 3.01$°A with the β¹-SiAlON peak intensity at $d = 3.2806$°. Similarly, relative amount of YbAG phase was given by dividing the YbAG peak intensity at the interplanar spacing of $d = 3.19$°A (I:25) with the β¹-SiAlON peak intensity at $d = 3.2806$°. Besides, to avoid misleading interpretations due to the different scattering capabilities of SiAlON and Jss, the I_{Jss}/I_β and I_{YbAG}/I_β ratios were only compared with the samples having similar α¹ and β¹ contents [16,19].

Fig. 3a,c,e,g,i shows as-sintered microstructures of α¹/β¹-SiAlON-TiN composites with different z value of β¹-SiAlON. The microstructure of the samples revealed the presence of four different contrasting phases. The prismatic grains with darker contrast were

β¹-SiAlON, the equiaxed grains with grey contrast were α¹-SiAlON, the grains with lighter grey shade were TiN and small white areas were intergranular phase due to the strong electron-scattering characteristic of the heavy metals. General microstructural features of the all materials are very similar except intergranular phase morphology. Z03, Z09 and Z11 samples had coalesced triple pockets as noticeable by larger pocket size. On the other hand, intergranular phase in Z05 and Z07 samples are generally distributed around the SiAlON grains. Z03 sample should have less aluminium and Z09 and Z11 should have higher aluminium in the intergranular phase. Z05 and Z07 should be in-between. What is more, substantial crystallization was observed only in Z03 (Fig. 1). These observations indicate that in the as-sintered samples, coalescence of the intergranular phase could be influenced by crystallization (Z03) and/or chemistry of the intergranular phase (Z05, Z07, Z09 and Z11).

3.2. The effect of post sintering heat treatment on crystallization of IGP

Table 3 presents the phase evolution, z values and IGP crystallization and Fig. 3b,d,f,h,j shows heat treated microstructures of α¹/β¹-SiAlON-TiN composites with different z value of β¹-SiAlON after post sintering heat treatment. The general microstructural features of the heat treated samples were very similar to the as-sintered samples (Fig. 3a,c,e,g,i). The only difference was observed in the coalescence behaviour. Despite some differences between the samples, all of them showed coalescence of the intergranular phase after heat treatment.

It was observed that Jss phase was still stable and its content did not change with heat treatment (after sintering I_{Jss}/I_β: 0.18, after heat treatment, I_{Jss}/I_β: 0.19) for Z03 sample (see Fig. 4). Microstructural investigations showed that the shape of triple junctions almost similar for sintered and heat treated Z03samples since both had similar extents of crystallization (Fig. 3a–b).

As stated before, with the increase in z value from 0.3 to 0.5, the amount of Jss phase content decreased for the sintered sample. After heat treatment of Z05 sample, Jss phase content was increasing and reached to the value of Z03 sample's Jss content (Fig. 4). Sintered Z05 sample had no good coalescence behaviour of the intergranular phase, but after heat treatment coalescence behaviour enhanced (Fig. 3c–d).

Sintered Z07 sample had low extent of intergranular phase crystallization (I_{Jss}/I_β: 0.027) with a Jss phase. After applying heat treatment, aluminate and Jss phases were observed to coexist but no substantial improvement in crystallization and a slight change in microstructure were obtained (see Fig. 3e–f). Among the materials with different z values, Z07 sample had the lowest crystallization and the worst coalescence behaviour. For Z09 sample, Jss phase was no longer stable with heat treatment and aluminate phase crystallization was obtained (Fig. 4). While weak aluminate phase peaks (I_a/I_β: 0.017) was observed after sintering, aluminate crystallization increased with heat treatment (I_a/I_β: 0.1) for Z11 sample (Fig. 4).

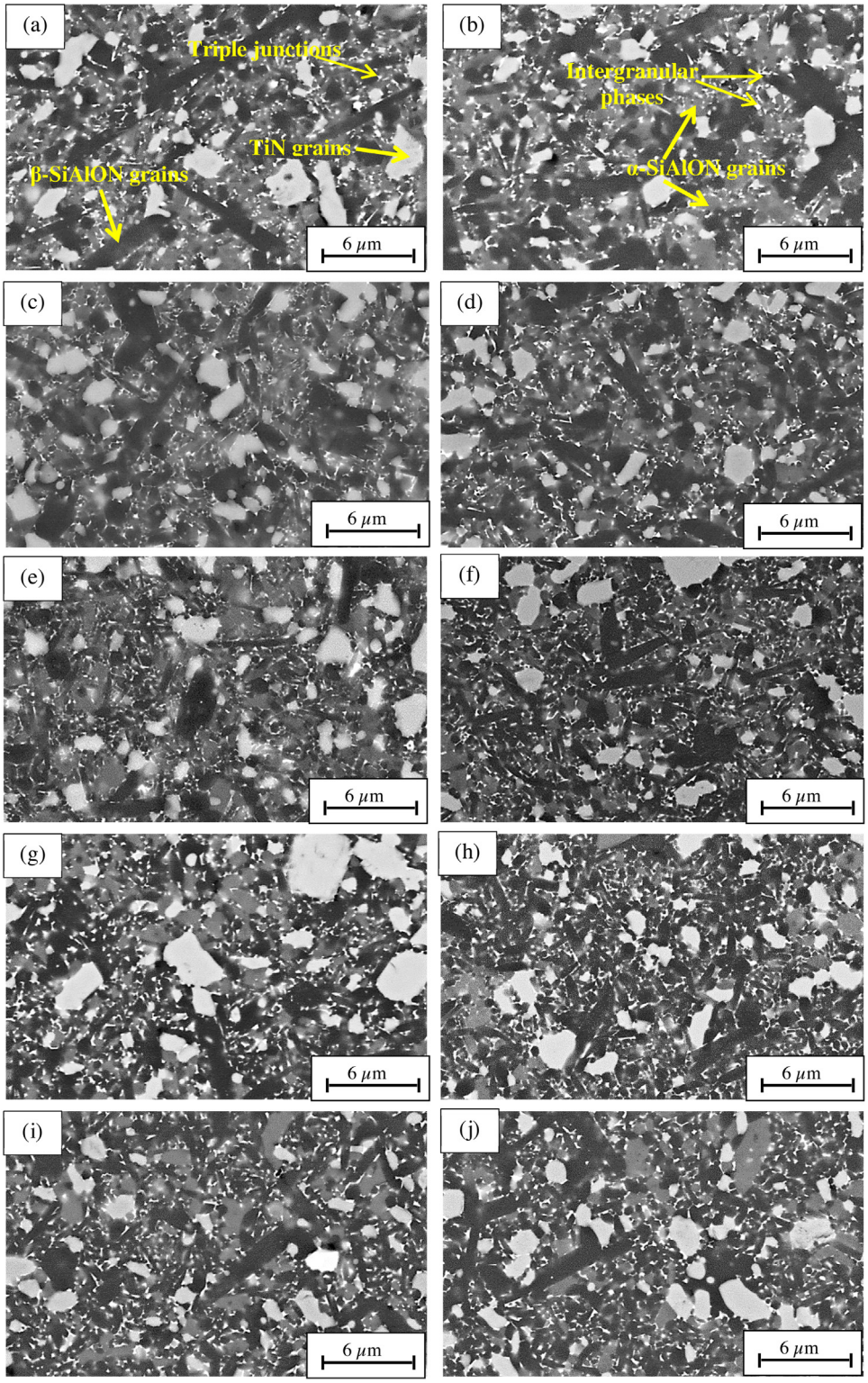

Fig. 3. Representative microstures of sintered and heat treated SiAlON-TiN composites with different z values (a) sintered and (b) heat treated Z03 sample, (c) sintered and (d) heat treated Z05 sample, (e) sintered and (f) heat treated Z07 sample, (g) sintered and (h) heat treated Z09 sample, (i) sintered and (j) heat treated Z11 sample.

3.3. *Effect of z value on mechanical properties*

The change in Vickers hardness and indentation fracture toughness values with different z values are given in Figs. 5 and 5, respectively. 3 samples tested for per composition with 5 indents. Standard deviation is changing between ±0.07 and 0.41 for hardness and 0.05 and 1.03 for fracture toughness. The standard deviation is the most for Z05 composition due to inhomogeneities in microstructure. After heat treatment more homogeneous microstructure was obtained and standard deviation decrease to 0.17.

Both the hardness and fracture toughness decreased with the increasing z values However, the changes were not significant. The hardness of SiAlON ceramics was controlled by mainly phase con-

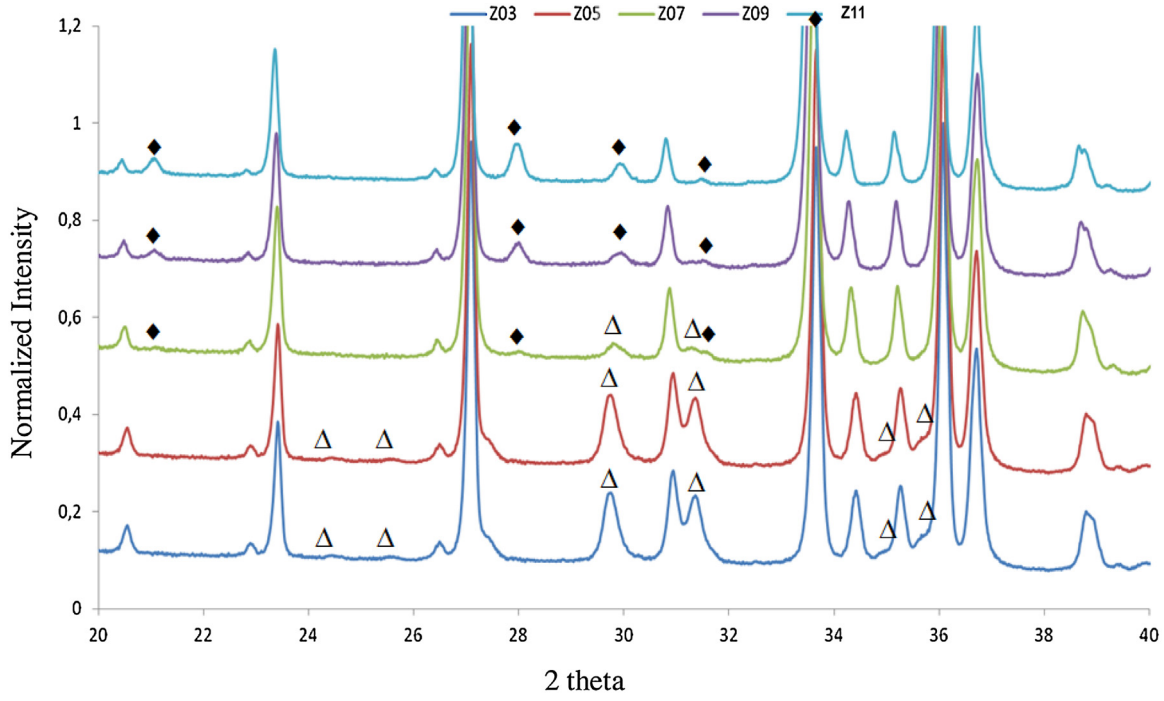

Fig. 4. XRD pattern of heat treated SiAlON-TiN composites which have different z values (Δ:Jss- $Yb_4Si_{2-x}Al_xO_{7+x}N_{2-x}$; ♦: $Yb_3Al_5O_{12}$).

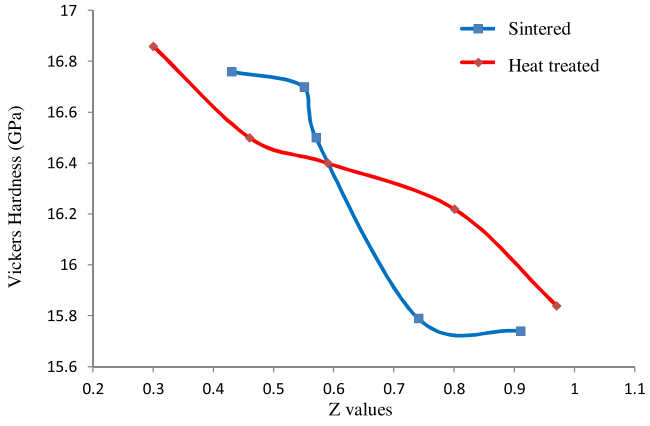

Fig. 5. Vickers hardness variations with change in z values.

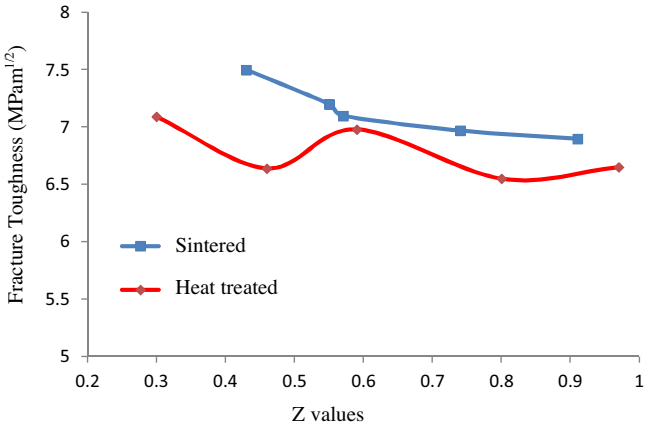

Fig. 6. Fracture toughness variations with change in z values.

tent. Microstructure (porosity, grain size, shape and orientations, second phase (s), z value etc.) also affects the hardness but it is less prominent than phase content. Therefore the hardness values of SiAlONs are narrowly varying between 15.74 GPa to 16.76 GPa, since the samples have similar α¹-SiAlON amount (23–29%), similar grain boundary phase nature (crystalline) and porosity level while different z values (0.43–0.91). Hardness increased with the increase in α¹-SiAlON phase content and decrease in z value. Z03 sample had the highest α¹-SiAlON amount (%29α) and lowest z value (0.43) and hence had the highest hardness value. On the other hand Z11 samples had the lowest hardness value due to the lowest α¹-SiAlON content (%23α) and the highest z value (0.91). Applying heat treatment to samples did not result in a significant increase in hardness values since α:β phase ratio almost kept constant and z values are nearly similar (Fig. 5).

Fracture toughness of SiAlON-TiN composites can be controlled by microstructure. Mainly grain morphology, bonding strength between the grain and grain boundary phases, nature of the IGP (crystalline or amorphous) and z value effect the fracture toughness. The fracture toughness values changes between the narrow range 7.5 and 6.9 $MPam^{1/2}$. Z03 sample had the highest fracture toughness value (7.5 $MPam^{1/2}$) since it had the lowest z value with elongated, high aspect ratio grains (Fig. 6). On the other hand, all samples have crystalline intergranular phase chemistry and probably had similar bonding strength between the grain and grain boundary phases and hence they have similar fracture toughness. Besides, thermal expansion coefficient mismatch between the SiAlON matrix ($3*10^{-6}/^{\circ}C$) and TiN ($9.4*10^{-6}/^{\circ}C$) reinforcement phase leads to microcracking which is major mechanism for the improvement in toughness of the composites. After heat treatment fracture toughness values a little bit decreased and the microstructure became coarser (Fig. 6). Vickers indents and crack lengths were measured with optical microscopy and the c/a ratio varied between 1.92-2.14. If the c/a ratio is low, crack propagation resistance will be high. These values indicated good crack propagation resistance for SiAlON-TiN composites. Fig. 7 shows the crack propagation behaviour of Z03, Z05 and Z11 composites. Crack deflection and crack bridging mechanisms were active for

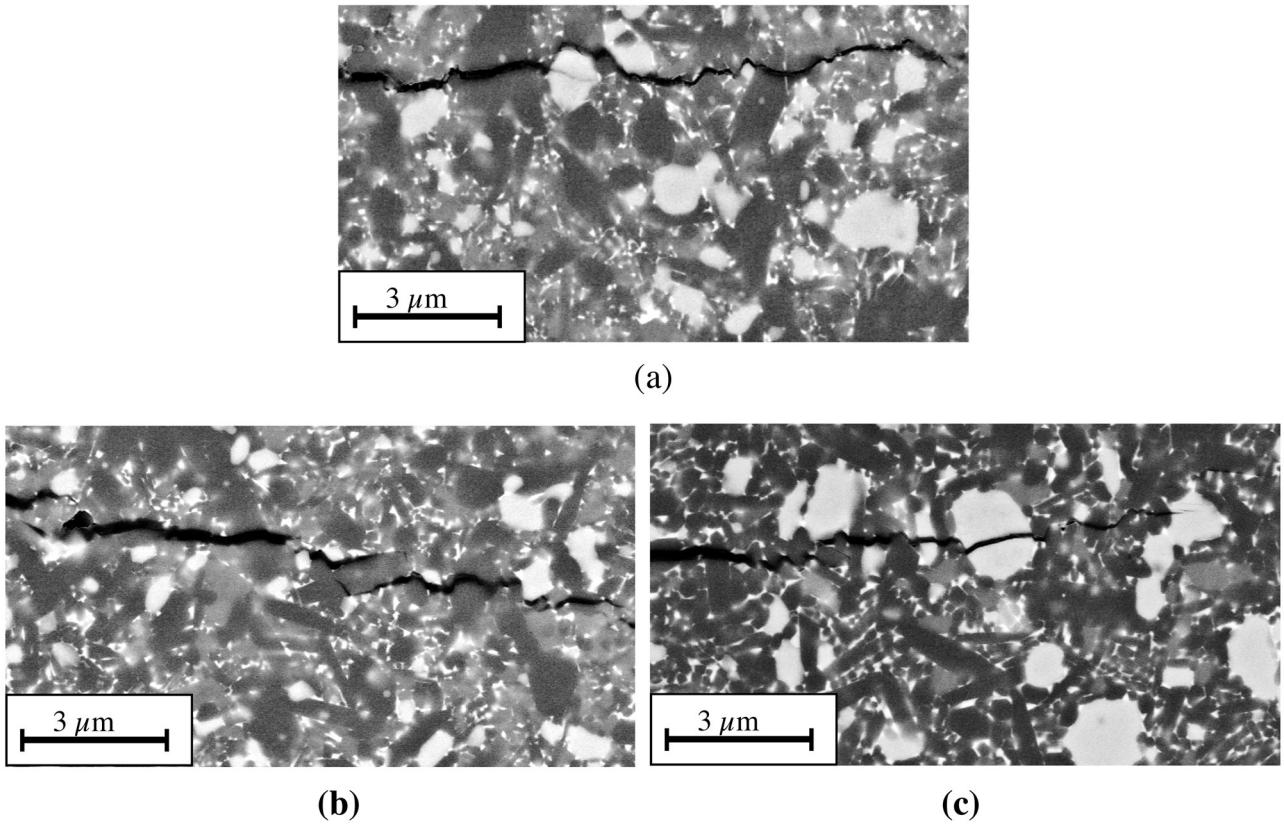

Fig. 7. Crack propagation behaviour of sintered (a) Z03, (b) Z0.5 and (b) Z11 samples taken by SEM-BSE mode.

improvement in fracture toughness. Grain morphology is effective to activate toughness mechanisms. Elongated β¹-SiAlON grains with smaller isometric α¹-SiAlON grains provides more complex possibilities for crack deflection and enhance fracture toughness. In particular, well developed elongated grains in Z03 and Z05 can lead to more effective crack bridging and deflection (see Fig. 7).

4. Conclusions

In this study, the effect of z value (between 0.3 to 1.1) of β¹-SiAlON on crystallization and coalescence behaviour of the intergranular phase was systematically investigated for sintered and heat treated α¹/β¹-SiAlON-TiN composites.

It was observed that z value was an effective parameter on intergranular phase chemistry and crystallization after sintering. Jss phase was predominantly stable when the z value was low (0.3-0.4). With the increase in z value over 0.74 crystallization tendency of the intergranular phase was decreased. With further increase in z value (>0.80) the stable phase was YbAG.

Post sintering heat treatment improved the crystallization and consequent coalescence was evident. Type of crystalline phase remained the same in sintered samples with low z values (0.3–0.55). With the increasing z value, crystallizing phase due to heat treatment changed from Jss phase to YbAG and the extent of YbAG crystallization improved with increasing z value. The hardness values changed between 16.86 ± 0.20 (for Z03) and 15.74 ± 0.07 (for Z11) and fracture toughness values changed between 7.50 ± 0.10 (for Z03) and 6.55 ± 0.05 for (Z09) in a narrow range since the samples have similar α¹:β¹ SiAlON phase ratio while different z value. The α¹:β¹ SiAlON phase ratio is more effective parameter than the z value on mechanical properties.

High z SiAlON-TiN composites which have excellent coalescence behaviour and crystallization of IGP and with satisfactory hardness and fracture toughness values making this composites interesting for use in cutting tool for superalloy machining.

Acknowledgement

This work was financially supported by TUBITAK (Ankara, Turkey) in the scope of CARIER-110M727 Project. (Project Manager: Assoc. Prof. Dr. Nurcan CALIS ACIKBAS).

References

[1] D.H. Jack, Ceramic cutting tool materials, Mater. Des. 7 (5) (1986) 267–273.
[2] W. Konig, K. Gerschwiler, Machining nickel-based superalloys, Manuf. Eng. 122 (3) (1999) 102.
[3] E.D. Whitney, Ceramic Cutting Tools, Noyes Publications, USA, 1994.
[4] E.O. Ezugwu, J. Bonney, Y. Yamane, An overview of the machinability of aeroengine alloys, J. Mater. Proc. Technol. 134 (2003) 233–253.
[5] E.O. Ezugwu, Z.M. Wang, A.R. Machado, The machinability of nickel-based alloys: a review, J. Mater. Process. Technol. 86 (1998) 1–16.
[6] T.C. Sims, S.N. Stoloff, C.W. Hagel, Süperalloys II, John Wiley&Sons, Canada, 1987.
[7] E.O. Ezugwu, Key improvements in the machining of difficult-to-cut aerospace superalloys, Int. J. Mach. Tool Manuf. 45 (2005) 1353–1367.
[8] J.D. Matthew, J.D. Stephen, Süperalloys, American Society for Metals, ASM International, USA, 2002.
[9] I.A. Choudhuryve, M.A. El-Baradie, Machinability of nickel-base super alloys: a general review, J. Mater. Process. Technol. 77 (1998) 278–284.
[10] H. Mandal, F. Kara, S. Turan, A. Kara, Novel SiAlON ceramics for cutting tool applications, Key Eng. Mater. 237 (2003) 193–202.
[11] L.J. Gauckler, H.L. Lukas, G. Petzow, Contribution to the phase diagram Si_3N_4-SiO_2-A1N-AI_2O_3, J. Am. Ceram. Soc. 58 (1975) 346–348.
[12] K.H. Jack, The significance of structure and phase equilibria in the development of silicon nitride and sialon ceramics, Sci. Ceram. 11 (1981) 125–142.
[13] T. Ekström, P.O. Köll, M. Nygren, P.O. Olssen, J. Mater. Sci. 24 (1989) 1853–1861.
[14] G. Brandt, Wear and Thermal Shock Resistant SiAlON Cutting Tool Material, U.S. Patent No. 5,965,471, 1999.

[15] P. K. Mehrotra, R. D. Nixon, J. L. Swiokla, High z SiAlON and Cutting Tools Made Therefrom and Method of Using, International Application Published Under the Patent Cooperation Treaty (PCT), WO 94/12317, 9 June, 1994.
[16] N. Calis Acikbas, O. Demir, The effect of cation type, intergranular phase amount and cation mole ratios on z value and intergranular phase crystallisation of SiAlON ceramics, Ceram. Int. 39 (2013) 3249–3259.
[17] N. Calis Acikbas, S. Tegmen, S. Ozcan, G. Acikbas, Thermal shock behaviour of α:β-SiAlON-TiN composites, Ceram. Int. 40 (2014) 3611–3618.
[18] F. Kara, H. Mandal, S. Turan, A. Kara, N.C. Acikbas, Development strategies for SiAlON ceramics, in: Global Roadmap for Ceramics ICC2 Proceedings, June 29–July 4 Toronto, 2008, pp. 119–128.
[19] N. Calis Acikbas, H. Yurdakul, H. Mandal, F. Kara, A.Kara S.Turan, B. Bitterlich, Effect of sintering conditions and heat treatment on the properties, microstructure and machining performance of α:β-SiAlON ceramics, J. Eur. Ceram. Soc. (2012) 1321–1327.
[20] K. Liddell, X-ray Analysis of Nitrogen Ceramic Phases MSc Thesis, University of Newcastle, Upon Tyne, UK, 1979.
[21] A.G. Evans, E.A. Charles, Fracture toughness determinations by indentation, J. Am. Ceram. Soc. 59 (1976) 371–372.
[22] K. Niihara, R. Morena, P.H. Hasselman, Evaluation of Kıc of brittle solids by the indentation method with low crack-to-indent ratios, J. Mater. Sci. Lett. 1 (1982) 13–16.
[23] V.A. Ijevskii, U. Kolitsch, H.J. Seifert, I. Wiedmann, F. Aldinger, Aluminium containing nitrogen woehlerite solid solutions. synthesis, structure, and some properties, J. Eur. Ceram. Soc. 18 (1998) 543–552.
[24] Z. Shen, T. Ekstrom, M. Nygren, Ytterbium stabilized α-SiAlON ceramics, J. Phys. D: Appl. Phys. 29 (1996) 893–904.
[25] K.S. Chee, Y.B. Cheng, E. Mark, The solubility of aluminum in rare earth nitrogen melilite phases, J. Eur. Ceram. Soc. 15 (1995) 1213–1220.
[26] C.P. Gazzara, D.R. Messier, Determination of phase content of Si3N4 by X-ray diffraction analysis, Am. Ceram. Soc. Bull. 56 (1977) 777–780.